

Molecular dynamics simulation studies on some topics of water molecules on hydrophobic surfaces

FANG Hai-Ping^{1,*} HU Jun^{1,2,*}

¹Shanghai Institute of Applied Physics, the Chinese Academy of Sciences, Shanghai 201800, China;

²Bio-X Life Sciences Research Center, College of Life Science and Technology, Shanghai Jiaotong University, Shanghai 200030, China)

Abstract Molecular dynamics simulations have been used to study two topics of water molecules on hydrophobic surfaces. Some properties of the nanobubbles with different ingredients and behavior of single water chains in single-walled carbon nanochannels are exploited. Molecular simulations show that the density of the N₂ and H₂ are quite high, which is critical for the stability of the nanobubbles and may have potential applications, such as hydrogen storage, incorporated with recent experimental method to controllably produce hydrogen nanobubbles. The water molecules inside the nanochannel show an unexpected directed motion with long time period, which is indispensable in the future study of the dynamics of biological channels.

Key words Molecular dynamics simulation, Nanobubble, Nanochannel

CLC numbers O485, O411.3

1 Introduction

Molecular dynamics simulations have been recognized as one of the most popular tools in the study of the behavior of systems at the nanoscale. Why water is so special and recognized as life matrix^[1] has long been discussed. And it is well known that hydrophobic force is one of the most important interactions in biological systems.^[2] This article will focus on two of the most often discussed problems: the nanobubbles and the water molecules permeation through nanochannels. Molecular dynamics simulations were used for this study.

2 Nanobubbles

Ten years ago, nanobubbles at the solid–water interface were proposed as an origin of the mysterious long-ranged attractive force as two hydrophobic surfaces approached each other in water.^[3] However,

conventional thermodynamics^[4] predicted that the lifetime of nanosize bubbles was only several picoseconds to hundreds of microseconds, which is too short to be observed experimentally. In recent years nanobubbles were directly observed by atomic force microscopy (AFM).^[5-11] Very recently, Zhang et al. have also found gas pancakes at the interface of water and HOPG (highly oriented pyrolytic graphite) by the exchange of ethanol and water.^[12] In 2003, Steitz et al. suggested that a precursor gas layer contributed to the depletion layer of D₂O, and nanobubbles were induced by the tip of AFM.^[13] Doshi et al. pointed out that the density reduction of water at the hydrophobic saline-water interface depended on the dissolved gases in water whereas preexisting nanobubbles were excluded.^[14] However, lately, Attard et al. insisted that nanobubbles are responsible for the long-ranged attractive force measured by AFM between hydrophobic surfaces immersed in water.^[15]

Partly supported by One-Hundred-Talent Project from the Chinese Academy of Sciences and Shanghai Supercomputer Center of China..

*E-mail: fanghaiping@sinap.ac.cn, jhu@sjtu.edu.cn

Received date: 2006-03-12

The importance of studying nanobubbles at the solid–water interface also lies in that, if there were nanobubbles at a hydrophobic solid–liquid interface, the dynamics of the system would be significantly changed, including the occurrence of a long-ranged interaction between hydrophobic interfaces immersed in water,^[3,16] the stability of colloidal systems,^[17] the flotation of minerals,^[18–20] the reduction of friction and drag in microfluidic transportation,^[21–23] and the rupture of wetting films.^[24] The existence and growth of nanobubbles on surface may have also profound potential influence and application in many important scientific fields such as fast protein folding and assembly,^[25–28] biosensors/biochips,^[29] detergent-free cleaning,^[30] ultrasound diagnostics, and local drug delivery in medicine.^[31]

With the rapid development of powerful computer facility, molecular dynamics simulation has been widely used in the study of the dynamics in the length scale of nanometers. Water vapor bubbles between two hydrophobic planar surfaces immersed in water and the collapse of water vapor bubbles in liquid have been studied by molecular dynamics.^[32,33] The former is stable while the lifetime for the latter is only about picoseconds. We will concentrate on the behavior of gas bubbles at the nanoscale filled with other ingredients, such as N₂ and H₂, in the water. We find that the densities of those gases in nanobubbles are considerably large.

The bond stretching interaction between two covalently bonded atoms *i* and *j* is represented by a harmonic potential:^[34]

$$V(r) = 1/2 k(r - b)^2$$

where *k* and *b* are force constant and standard bond length of harmonic potential; the values are defined in Gromacs Manual 3.2.^[34]

The interactions between molecules are expressed by the Lennard–Jones potential function:

$$\varphi = 4\xi \left[\left(\frac{\sigma}{r} \right)^{12} - \left(\frac{\sigma}{r} \right)^6 \right]$$

where σ and ξ are the length scale and the energy scale of the Lennard–Jones potential, respectively. Universal Force Field parameters^[35] are used in our simulation. The parameters used in simulations are

$$b_N = 0.1120 \text{ nm}, k_N = 1,280,025 \text{ kJ}\cdot\text{mol}^{-1}\cdot\text{nm}^{-2},$$

$$\xi_N = 289 \text{ J}\cdot\text{mol}^{-1}, \sigma_N = 0.326 \text{ nm}; b_H = 0.0708 \text{ nm}, k_H = 758,921 \text{ kJ}\cdot\text{mol}^{-1}\cdot\text{nm}^{-2}, \xi_H = 184 \text{ J}\cdot\text{mol}^{-1}, \sigma_H = 0.0392 \text{ nm}.$$

The other parameters used in this article, including the interactions between water molecules, are set according to Gromacs 3.2.1^[34] and the SPC^[36] water mode is adopted.

2.1 Simulations of N₂

We begin with the simulation of N₂. We have simulated two kinds of systems. The molecule dynamics simulations were carried out at a constant pressure (0.1 MPa) and at constant temperature with Gromacs 3.2.1. Periodic boundary conditions are applied in all directions. The time step is 0.002 ps.

2.1.1 Molecular simulation of liquid droplet N₂ at 77.3K

In our series of simulations, the systems contained N₂ molecules, the numbers of which are 1024, 1500, and 2048, respectively. The initial box size is $L_x = 12 \text{ nm}$, $L_y = 10 \text{ nm}$, $L_z = 10 \text{ nm}$. That the system was believed to reach the equilibrium when we got a constant density independent of time. Initially, nitrogen molecules formed a simple cubic structure, with a lattice constant $1.8405 \sigma_N$. The data were collected after 1-ns simulation.

The local density at a distance *r* from the center is calculated in a spherical shell with a small width of 0.2 nm. The result is shown in Fig. 1. By fitting a tanh function,^[37] the densities at the center of the liquid droplet are 829, 812, and 816 kg·m⁻³ for $N = 2048$, 1500, and 1024, respectively. Those values

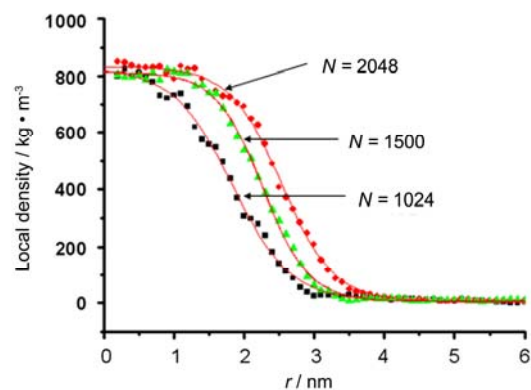


Fig.1 Local density profiles for different numbers of N₂ molecules. The squares, diamonds, and triangles are the simulation results while the lines are the fit tanh functions.

are very close to the experimental value of $807.4 \text{ kg}\cdot\text{m}^{-3}$ at the boiling temperature, 77.3 K [38] and a pressures of 0.1 MPa . This verifies the method of our simulations.

2.1.2 Molecular simulation of N_2 bubbles immersed in water at room temperature

The computation box in our simulations has the size of $L_x = 14 \text{ nm}$, $L_y = 10 \text{ nm}$, $L_z = 10 \text{ nm}$. The system contains 1600 nitrogen molecules and 43,915 water molecules. Initially, nitrogen molecules in a simple cubic structure are located in the center of the box, with a lattice constant $1.8405 \sigma_{\text{N}}$. The data were collected at 1 and 1.5 ns, respectively. We found that the results for different times are quite similar so we believe that the system has reached the equilibrium.

The local densities are shown in Fig. 2. By fitting to a tanh function, [37] our simulation result shows that the density at the center of the nanobubble is $260 \text{ kg}\cdot\text{m}^{-3}$ at room temperature and a pressure of 0.1 MPa .

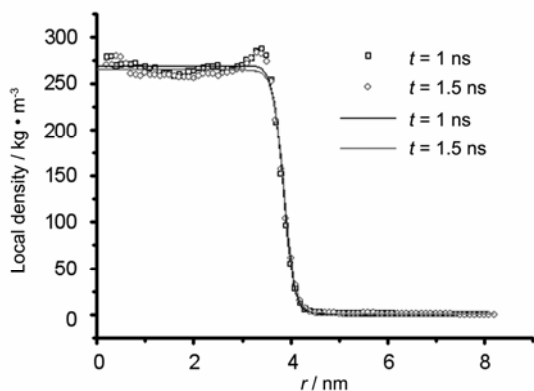


Fig.2 Local density profiles of a N_2 nanobubble in water. The open squares and diamonds are the simulation results while the lines are the fit tanh functions.

2.2 Simulations of H_2

We also simulated simulations on two kinds of systems. The molecule dynamics simulations were carried out at a constant pressure (0.1 MPa) and constant temperature with Gromacs 3.2.1. Periodic boundary conditions are applied in all directions. The time step is 0.002 ps .

2.2.1 Molecular simulation of liquid droplet H_2 at temperature 22 K

The computation box in our simulations has the size of $L_x = 10 \text{ nm}$, $L_y = 10 \text{ nm}$, $L_z = 10 \text{ nm}$. Our simulations contain a system with a temperature of $T = 22 \text{ K}$. The system was believed to reach the equilibrium

when a constant density, independent of time, was reached. Initially, hydrogen molecules formed a simple cubic structure, with a lattice constant $15.3 \sigma_{\text{H}}$. The data were collected after 1 ns simulation.

The local density profile is shown in Fig. 3. By fitting to a tanh function, [37] the density at the center of the liquid droplet was $78.6 \text{ kg}\cdot\text{m}^{-3}$ at $T = 22 \text{ K}$. Those values are close to the experimental value of $70.9 \text{ kg}\cdot\text{m}^{-3}$ at boiling temperature 22 K [39] and pressure of 0.1 MPa .

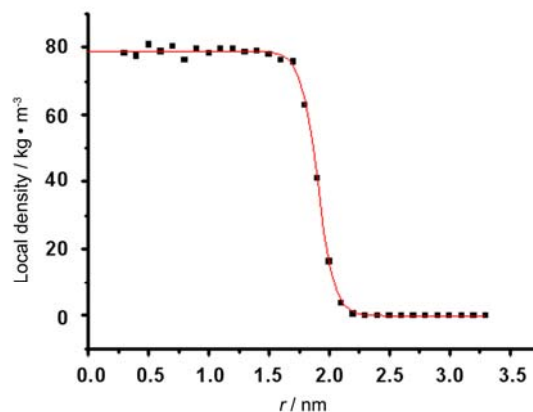


Fig.3 Local density profile of H_2 at boiling temperature 22 K . The squares are the simulation results while the line is the fit tanh function.

2.2.2 Molecular simulation of H_2 bubbles immersed in water at room temperature

The computation box in our simulations has the size, $L_x = 10 \text{ nm}$, $L_y = 10 \text{ nm}$, $L_z = 10 \text{ nm}$. The system contains 1728 hydrogen molecules and 29,037 water molecules. Initially, hydrogen molecules in a simple cubic structure were solved in the center of the box, with a lattice constant $15.3 \sigma_{\text{H}}$. The data were collected after 1 ns simulation. The results for different times were found to be quite similar, leading to the conclusion that the system has reached the equilibrium.

The local density profiles are shown in Fig. 4. By fitting to a tanh function, [37] our simulation result shows that the density at the center of the H_2 nanobubbles is $10.9 \text{ kg}\cdot\text{m}^{-3}$ at room temperature and a pressure of 0.1 MPa .

From the simulations we found that the density in gas bubble is quite high, i.e. 32% of the density of liquid N_2 and 14% of liquid H_2 . This is unexpected. Further studies are necessary to clarify whether the MD simulation results really reflect the real cases.

Moreover, if the high density is confirmed, the name nanobubble may be not appropriate. However, in this article, we still call it gas nanobubble.

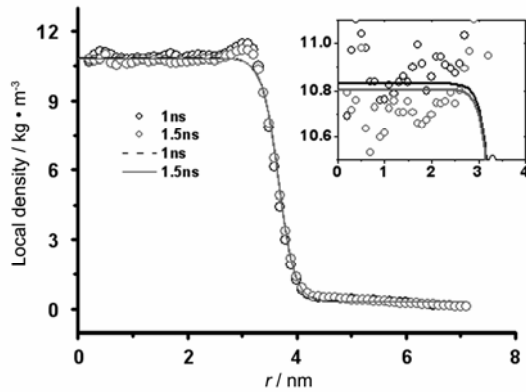


Fig.4 Density profile of H_2 nanobubbles immersed water. Inset is an enlarged part at $r \rightarrow 0$. The circles are the simulation results while the lines are the fit tanh functions.

Previously, MacLeod and Sugden had suggested an empirical relationship between surface tension and density.^[40]

$$\gamma = [P(\rho_L - \rho_V)/M]^4$$

where γ is the surface tension, P is the parachor of the liquid, ρ_L and ρ_V are the liquid and the vapor densities ($g \cdot cm^{-3}$), respectively, and M is the molecular weight of the liquid. If the equation can be applied to this study of the nanobubbles, and the gas accumulated at the liquid/solid interface at the nanoscale has high density as indicated by the MD simulations, the surface tension will greatly reduce, i.e., if the density of the gas state is 20% of the density of water, the surface tension is only 40% of the original value ($72 \text{ mN} \cdot \text{m}^{-1}$). The stability difficulty due to the huge pressure might disappear. More detailed study of the nanobubble stability will be presented elsewhere. Moreover, the simulation results also give a possible suggestion for potential applications of gas with high density. In fact, recently, hydrogen nanobubbles were also controllably produced on graphite surface using electrochemical approach. The coverage of gas bubbles or gas pancakes can be as large as 90% of the surface. If the gas density is 20% of the density of water, hydrogen nanobubbles with high coverage rates can be used as a new matter for hydrogen storage at room temperature and ambient atmosphere pressure.^[41]

3 Water molecules permeation across nanochannels

One of the motivations of studying water molecules permeation across nanochannels comes from the problems in biological membrane transportation.^[42-46] Since the first atomic resolution of the aquaporins by Agre et al., much attention has been paid on how the behavior of water molecules depends on the shape and dimension of nanochannels.^[47] Molecular dynamics simulation is one of the most important tools in this direction. Despite the efforts on the direct simulations on water permeations across the biological channels such as Aquaporin, Glpf and MscS,^[46, 48-51] simple model channels have been widely used to exploit primary characteristics of those biological channel, considering the complicated structure of membranes and membrane–water interactions. The study of the model nanochannels is also useful for the future development of nanodevice. In 2001, Hummer et al. showed that single-walled carbon nanotubes (SWNT) could be designed to be molecular channels for water.^[52] They observed that a minute reduction in the attraction between the tube wall and water dramatically affected pore hydration, leading to sharp, two-state transitions between empty and filled states on a nanosecond timescale.^[52] Beckstein et al. have investigated the passage of water through atomistic models of hydrophobic nanopores embedded in a membrane mimetic by molecular dynamics simulations.^[53] An abrupt transition from a closed state (no water in the pore cavity) to an open state (trapped water at approximately bulk density) has been found once a critical pore radius is exceeded.^[53] The vapor–liquid transition has also been observed in mechanosensitive channels^[51, 54, 55] and other hydrophobic nanopores.^[55-58]

The single-file water molecules in those nanochannels have been observed for a long time. Recent studies show that many of the special properties of those systems result from the nearly-aligned single-file water molecules. In our previous studies, we have studied the behavior of water molecules in a SWNT with 8.1 \AA in diameter and 13.1 \AA in length under deformations^[59] and electric signals. It has been found that the system is both effectively resistant to deformation/electric noises and sensitive to available sig-

nals.^[59] The average number of water molecules distributed inside the channel is about 5. There is a clear wavelike pattern of the water molecules and we found that it plays an important role in the high deformation signal-to-noise ratio.^[59] However, when the length of a SWNT increases a little, say by 1.2 Å, the average number of water molecules inside approaches 5.5 so that the wavelike pattern is not clear. This article will focus on some properties of the nearly aligned water chain in this SWNT.

The simulation framework is shown in Fig. 5. A single graphite sheet divided the full space into two parts. To mimic the biological water channels in membranes, an uncapped, single-walled carbon nanotube, 14.6 Å in length and 8.1 Å in diameter, along the z -direction was embedded in the center of a graphite sheet. The single graphite sheet divided both the full space and the SWNT into two equal parts. The 156-carbon (6,6) nanotube was formed by folding a graphite sheet of 5×12 carbon rings to a cylinder, and then relaxed with the interaction between carbon atoms. This interaction was described with the parameterized potential by Brenner^[60] according to the Tersoff formulism.^[61] Initially, water molecules were filled in the other space of the system except for the channel of the SWNT. Periodic boundary conditions were applied in all directions.

The molecule dynamics simulations were carried out at a constant pressure (0.1 MPa with initial box size $L_x = 3.0$ nm, $L_y = 3.0$ nm, $L_z = 4.0$ nm) and temperature (300 K) with Gromacs 3.2.1.^[34] Here the TIP3P^[62] water model was applied. A time step of 2 fs was used and data were collected every 0.5 ps. In the simulations, the carbon atoms were modeled as uncharged Lennard–Jones particles with a cross-section of $\sigma_{CC} = 0.34$ nm, $\sigma_{CO} = 0.3275$ nm, and a depth of the potential well of $\varepsilon_{CC} = 0.3612$ kJ·mol⁻¹, $\varepsilon_{CO} = 0.4802$ kJ·mol⁻¹.^[52] Carbon–carbon bond lengths of 0.14 nm and bond angles of 120° were maintained by harmonic potentials with spring constants of 393,960 kJ·mol⁻¹ nm⁻² and 527 kJ·mol⁻¹·(°)⁻² before relaxation.^[59] In addition, a weak dihedral angle potential was applied to bonded carbon atoms.^[63]

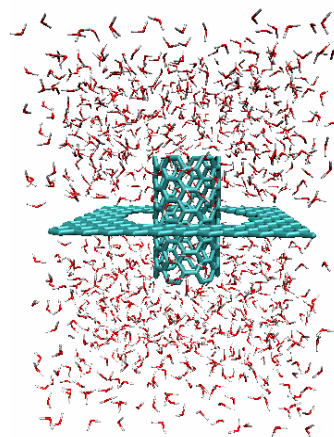


Fig.5 Snapshot of the simulation system.

The carbon nanotube together with the graphite sheet solvated in a water reservoir was simulated for 122 ns using molecular dynamics and the results in the last 120 ns were collected for analysis. The average number of water molecules is 5.4. In Fig. 6, the distribution of water molecules inside the nanotube along the z -direction is shown. Unlike that in a SWNT with a length of 13.1 Å, the wavelike pattern is negligible.

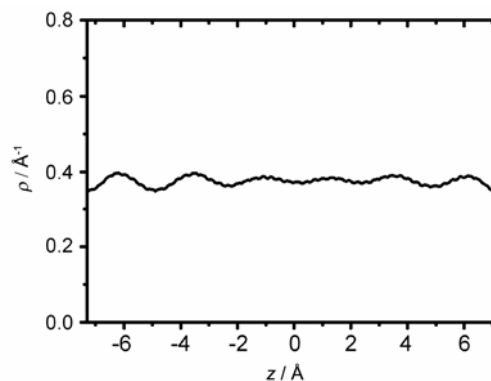


Fig.6 Water distribution along the nanotube axis.

Hydrogen bonds in the SWNT are highly oriented and nearly aligned with the nanochannel axis and collectively flip in their orientations.^[52, 64] In our previous article, we tried to quantify the orientation of water chain by defining a characteristic angle denoted by $\bar{\phi}$.^[58] The variable ϕ is the angle between a water molecule dipole and the z -axis, and the average runs over all the water molecules inside the nanochannel. It is found that $\bar{\phi}$ usually falls in two ranges, $15^\circ < \bar{\phi} < 50^\circ$ and $130^\circ < \bar{\phi} < 165^\circ$, which were called + dipole and – dipole states, respectively.^[59] In Fig. 7, we show the probabilities of the water fluxes for + dipole and – dipole states. We find that the net flux usually has the same direction with the dipole

orientation of the hydrogen-bonded chain inside the SWNT. The average duration for each state is 3.1 ns. For each state with duration larger than 1 ns, the data are collected for further analysis. We obtained a total of 57 ns in + dipole state and 35 ns in - dipole state from the simulation. The average net fluxes are 4.9 ns^{-1} and -3.9 ns^{-1} along the $+z$ -axis for + dipole and - dipole states, respectively.

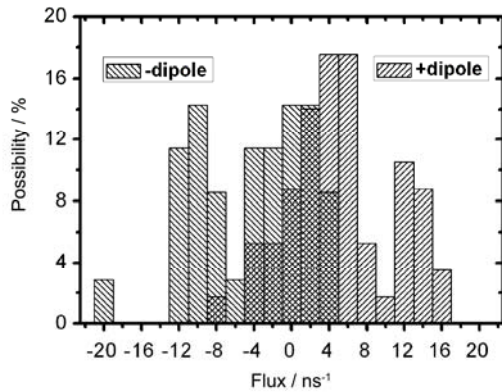


Fig.7 Probabilities of the water fluxes for + dipole and - dipole states.

Why is there net flux for each state? It is clear that the SWNT is electrically neutral and the polarization of the carbon atoms by the hydrogen bond has not been included. In 2004, Kosztin and Schulten have shown that the asymmetry of potential of mean force (PMF) can result in the transporting of glycerol molecules across the membrane even against the concentration.^[64] The PMF for water molecules for + and - dipole states are shown in Fig. 8(a). We can find a systematic difference between them, which can be seen more clearly in Fig. 8(b). The PMF for each state is also asymmetric. Consequently, the net flux of water can be expected from the theory of Kosztin and Schulten.

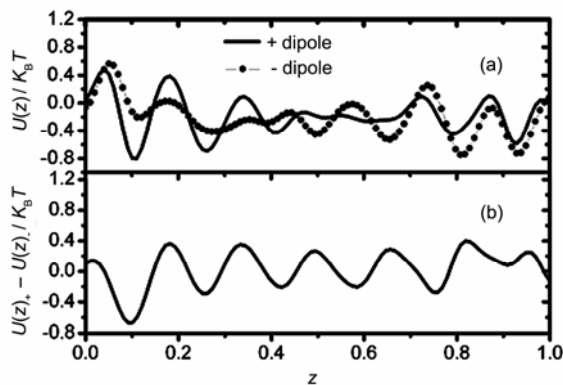


Fig.8 (a) The potential of mean force $U(z)_{\pm}$ of water molecules inside a SWNT for + dipole and - dipole states, z is the normalized position in the nanotube along the z -direction. (b) $U(z)_{-} - U(z)_{+}$.

Following three points should be noted: (1) The time duration for such transportation of water is still short while that for glycerol transporting in Ref. [64] can be infinity. However, since the asymmetry of the PMF in Ref. [64] is due to the asymmetrical structure of the aquaglycerol channel protein, without an external force, it is quite difficult to keep the asymmetrical structure. In the present system, the structure of the SWNT is completely symmetrical. The duration can be long for a long SWNT. (2) The present system is not a perpetual motion machine since the duration for net water transportation is limited. If we have a time-scale much higher than the duration, each state is only an orientation fluctuation. The average net flux approaches zero when the timescale approaches infinity. However, if we have an elegant trigger, useful work can be gained in the time interval within each orientation fluctuation state. (3) The net flux in each state is comparable to the biological value,^[45] showing that this mechanics is important in the study of the biological systems.

Acknowledgments

The authors thank Mr. Chunlei Wang and Hangjun Lu for preparing several data and figures of the manuscript. Zhaoxia Li and Lijuan Zhang are also acknowledged for revising some parts of the manuscript.

References

- 1 Ball P. Cellular and Molecular Biology, 2001, **47**: 717-720.
- 2 Ashbaugh H S, Pratt L R. Rev. Mod. Phys., 2006, **78**: 159-178.
- 3 Parker J L, Caisson P M, Attar P. J. Phys. Chem., 1994, **98**: 8468-8480.
- 4 Ljunggren S, Eriksson J C. Colloids and Surf. A, 1997, **129/130**: 151-155.
- 5 Ishida N, Inoue T, Miyahara M, *et al.* Langmuir, 2000, **16**: 6377-6380.
- 6 Lou S T, Ouyang Z Q, Zhang Y, *et al.* J. Vac. Sci. Technol. B, 2000, **18**: 2573-2575.
- 7 Lou S T, Gao J X, Xiao X D, *et al.* Chin. Phys., 2001, **10**: 108-110.
- 8 Tyrrell J W G, Attard P. Phys. Rev. Lett., 2001, **87**: 176104.
- 9 Attard P, Moody M P, Tyrrell J W G. Physica A, 2002, **314**: 696-705.
- 10 Yang J W, Duan J M, Fornasiero D, *et al.* J. Phys. Chem. B, 2003, **107**: 6139-6147.
- 11 Attard P. Adv. Colloid Interface Sci. 2003, **104**: 75-91.
- 12 Zhang X H. Studies of nanobubbles at solid/liquid interface, PhD Thesis. Shanghai Jiaotong University, 2004.
- 13 Steitz R, Gutberlet T, Hauss T, *et al.* Langmuir, 2003, **19**:

- 2409-2418.
- 14 Doshi D A, Watkins E B, Israelachvili J N, *et al.* Proc. Natl. Acad. Sci. USA, 2005, **102**: 9458-9462.
- 15 Stevens H, Considine R F, Drummond C. J, *et al.* Langmuir, 2005, **21**: 6399-6405.
- 16 Carambassis A, Jonker L C, Attard P, *et al.* Phys. Rev. Lett., 1998, **80**: 5357–5360.
- 17 Nguyen A V, Evans G M, Nalaskowski J, *et al.* Experimental Thermal and Fluid Science, 2004, **28**: 387–394.
- 18 Du Z P, Montoya M P B, Binks B P, *et al.* Langmuir, 2003, **19**: 3106–3108.
- 19 Ralston J, Fornasiero D, Mishchuk N. Colloids and Surf. A, 2001, **192**: 39–51.
- 20 Nguyen A V, Nalaskowski J, Miller J D. J. Colloid Interface Sci., 2003, **262**: 303–306.
- 21 Vinogradova O I. Langmuir, 1995, **11**: 2213–2220.
- 22 Granick S, Zhu Y X, Lee H J. Nature Materials, 2003, **2**: 221–227.
- 23 de Gennes P G. Langmuir, 2002, **18**: 3413–3414.
- 24 Stöckelhuber K W, Radoev B, Wenger A, *et al.* Langmuir, 2004, **20**: 164–168.
- 25 Zhou R H, Huang X, Margulis C J, *et al.* Science, 2004, **305**: 1605–1609.
- 26 Liu P, Huang X, Zhou R H, *et al.* Nature, 2005, **437**: 159–162.
- 27 ten Wolde P R, Chandler D. Proc. Natl. Acad. Sci. USA, 2002, **99**: 6539–6543.
- 28 Ball P. Nature, 2003, **423**: 25–26.
- 29 Holmberg M, Kuhle A, Garnæs J, *et al.* Langmuir, 2003, **19**: 10510–10513.
- 30 Pashley R M, Rzechowicz M, Pashley L R, *et al.* J. Phys. Chem. B, 2005, **109**: 1231–1238.
- 31 Lohse D. Phys. Today, 2003, **56**: 36-39.
- 32 Koishi T, Yoo S, Yasuoka K, *et al.* Phys. Rev. Lett., 2004, **93**: 185701.
- 33 Francesca L, Siegfried H, Francesco Z. J. Am. Chem. Soc., 2005, **127**: 8020.
- 34 Van der Spoel D, Lindahl E, Hess B, *et al.* Gromacs-3.2.1, Department of Biophysical Chemistry, University of Groningen, 2004; www.gromacs.org.
- 35 Rappe A K, Casewit C J, Colwell K S, *et al.* J. Am. Chem. Soc., 1992, **114**: 10024-10035.
- 36 Berendsen H J C, Postma J P M, van Gunsteren W F, *et al.* in Intermolecular forces, ed. Pullman B. (Reidel: Dordrecht, The Netherlands), 1981: 331–342.
- 37 Maruyama S, Matsumoto S, Shoji M, *et al.* Thermal Science and Engineering, 1994, **2**: 77.
- 38 <http://www.tkb-4u.com/articles/consumables/whatisnitrogen/whatisnitrogen.php>.
- 39 <http://www.speclab.com/elements/hydrogen.htm>
- 40 Poling B. E, Prausnitz J M, O'Connell J P. The properties of gases and liquids, McGraw-Hill Professional, 2000.
- 41 Zhang L J, Hu J, Fang H P, *et al.* Novel method and integrative apparatus of production and storage of hydrogen, China Inventive Patent, Application Number: 200510111758.3
- 42 Denker B M, Smith B L, Kuhajda F P, *et al.* Biol. Chem., 1988, **263**: 15634-15642.
- 43 Preston G M, Agre P. Proc. Natl. Acad. Sci. USA, 1991, **88**: 11110-11114.
- 44 Murata K, Mitsuoka K, Hirai T, *et al.* Nature, 2000, **407**: 599-605.
- 45 Zeidel M L, Ambudkar S V, Smith B L, *et al.* Biochemistry, 1992, **31**: 7436-7440.
- 46 de Groot B L, Grubmüller H. Science, 2001, **294**: 2353-2357.
- 47 Finkelstein A, Water movement through lipid bilayers, pores, and plasma membranes: Theory and reality, Wiley: New York, 1987.
- 48 Tajkhorshid E, Nollert P, Jensen M Ø, *et al.* Science, 2002, **296**: 525-530.
- 49 Vidossich P, Cascella M, Carloni P. Protein, 2004, **55**: 924-931.
- 50 Zhu F Q, Tajkhorshid E, Schulten K. Biophys. J., 2004, **86**: 50-57.
- 51 Anishkin A, Sukharev S. Biophys. J., 2004, **86**: 2883-2895.
- 52 Hummer G, Rasalah J C, Noworyta J P. Nature, 2001, **414**: 188-190.
- 53 Beckstein O, Biggin P C, Sansom M S P A. J. Phys. Chem. B, 2001, **105**: 12902-12905.
- 54 Saparov S M, Pohl P. Proc. Natl. Acad. Sci. USA, 2004, **101**: 4805-4809.
- 55 Biggin P C, Sansom M S P. Curr. Biol., 2003, **13**: R183-R185.
- 56 Maibaum L, Chandler D J. Phys. Chem. B, 2003, **107**(5): 1189-1193.
- 57 Beckstein O, Sansom M S P. Proc. Natl. Acad. Sci. USA, 2003, **100**: 7063-7068.
- 58 Grubmuller H. Proc. Natl. Acad. Sci. USA, 2003, **100**: 7421-7422.
- 59 Wan R. Z, Li J Y, Lu H J, *et al.* J. Am. Chem. Soc., 2005, **127**: 7166-7170.
- 60 Brenner D W. Phys. Rev. B, 1990, **42**: 9458-9471.
- 61 Tersoff J. Phys. Rev. Lett., 1988, **61**: 2879-2882.
- 62 Jorgensen W L, Chandrasekhar J, Madura J D, *et al.* J. Chem. Phys., 1983, **79** (2): 926-935.
- 63 Van der Spoel D, Lindahl E, Hess B, *et al.* Gromacs User Manual 3.1.1, Department of Biophysical Chemistry, University of Groningen, 2002.
- 64 Kosztin I, Schulten K. Phys. Rev. Lett., 2004, **93**: 238102.